



1 **Rising Lake Levels Across High Mountain Asia**

2 Javed Hassan¹, Karina Nielsen¹, William Colgan², Rijan Bhakta Kayastha³, Mira Khadka⁴,
3 Shfaqat Abbas Khan¹

4 ¹DTU Space, Technical University of Denmark, Kgs. Lyngby, 2800, Denmark.

5 ²Department of Glaciology and Climate, Geological Survey of Denmark and Greenland,
6 Copenhagen, 1350, Denmark.

7 ³Department of Environmental Science and Engineering, Himalayan Cryosphere, Climate and
8 Disaster Research Center (HiCCDRC), School of Science, Kathmandu University, Dhulikhel,
9 6250, Nepal.

10 ⁴Climate Cubit, Kathmandu, 44600, Nepal.

11 *Correspondence to:* Javed Hassan (javed@space.dtu.dk)

12 **Abstract**

13 High-altitude lakes across High Mountain Asia (HMA) are one of the critical freshwater
14 reservoirs and sensitive indicators of climate change due to their remote locations and limited
15 human disturbances. This study presents continuous water level estimates for 232 lakes across
16 HMA from 2010 to 2024 using CryoSat-2 and ICESat-2 data. We analyzed temporal and spatial
17 variations and inter-mission consistency in the lake water level across HMA. Our results reveal
18 an overall increasing trend (median rate: $+0.1 \pm 0.01$ m yr⁻¹), with 77% of lakes experiencing
19 rising levels and 91% exhibiting statistically significant trends. We find a substantial regional
20 heterogeneity with the Tibetan Plateau contributing dominantly to regional increase ($0.07 \pm$
21 0.001 m yr⁻¹), while Himalayan lakes show persistent decline (0.04 ± 0.001 m yr⁻¹). Water level
22 times series observed with the satellite altimetry missions CryoSat-2 and ICESat-2
23 intercomparison demonstrates strong consistency (80% sign agreement, $p = 0.013$). Lake
24 catchment scale analysis identifies precipitation as the dominant driver of lakes water level
25 variability ($r = 0.42$, $p < 0.001$), whereas lakes in glaciated catchments exhibit weak climate
26 correlations despite significant increases in temperature, indicating nonlinear cryosphere
27 buffering. We find systematic relationships between lake characteristics (area, elevation) and
28 increasing water levels, with larger lakes generally showing more rapid growth. The
29 contrasting hydrological responses with continued rising water levels in cryosphere influenced
30 lakes and accelerating declines in precipitation sensitive lakes in Himalaya highlight divergent
31 lake hydrological regimes. These findings underscore the critical importance of regional
32 differentiation in understanding lake water storage changes and informing climate adaptation
33 strategies for population vulnerable to these changes in the regions.

34 **Key words:** High Mountain Asia, Lake level change, satellite altimetry, climate change



35 1. Introduction

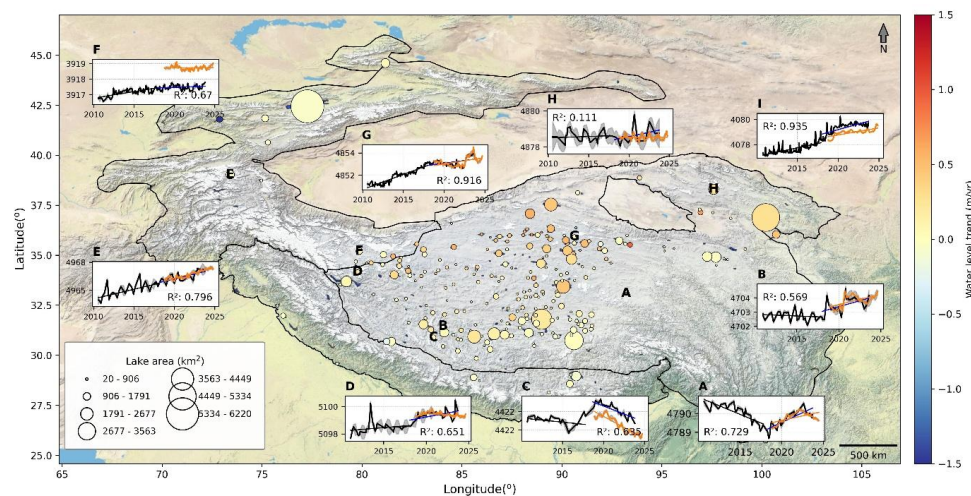
36 The remote location and limited human disturbances of high-altitude lakes across High
37 Mountain Asia (HMA) serve as sensitive indicators of climate change. In these data scarce
38 regions, lake water level fluctuations offer essential constraints on catchment water storage and
39 the evolving regional hydrological cycle (Lei et al., 2014; Pekel et al., 2016; Woolway et al.,
40 2020). The HMA, often termed as the “Third Pole” has undergone rapid warming particularly
41 the Tibetan Plateau (0.50-0.67°C/decade) in recent decades (Kuang and Jiao, 2016; Niu et al.,
42 2021; Wu et al., 2023), with rates exceeding the global average (Duan and Xiao, 2015)
43 contributing to accelerating glacier mass loss (Hugonnet et al., 2021; Zemp et al., 2025) and
44 reduced snow persistence (Muhammad, 2024), along with precipitation changes (Na et al.,
45 2024; Ouyang et al., 2020). Lakes within the region integrate these interacting processes,
46 understanding their long-term behavior is essential to quantify the hydrological response and
47 associated risks. This, in turn, has affected seasonal water availability in mountainous regions
48 and has contributed to expansion of nearby lakes (Miles et al., 2021; T Zhang et al., 2023).

49 The pronounced increase in water levels of endorheic and glacial lakes in HMA has been
50 evident in recent studies (Song and Sheng, 2016; Zhang et al., 2017b; Zhang et al., 2023), and
51 attributed to both increase in precipitation and cryosphere melt (Lei et al., 2014; G Zhang et
52 al., 2017b). In the meantime, since 1990, glacial lakes in the region have increased rapidly in
53 both number and size (Shugar et al., 2020), heightening the risk of glacial lake outburst flood
54 hazards for ~1 million people living within the immediate vicinity (Taylor et al., 2023). These
55 changes underscore a need for continuous monitoring of lake water level changes, both as
56 critical freshwater resources and hazards (Immerzeel and Bierkens, 2012; Zheng et al., 2021).
57 Snow and ice melt contributions to lake volume change on the Tibetan Plateau is estimated to
58 be limited and primarily driven by precipitation (Brun et al., 2020). Extreme precipitation
59 anomalies previously lead to abrupt lake level changes on Tibetan Plateau (Lei et al., 2019;
60 Song and Sheng, 2016). In-situ monitoring of these high-altitude lakes is logistically
61 challenging, which limits the number of in-situ observations (Lei et al., 2017). On the regional
62 scale, water level estimates in high-altitude lakes across HMA have been derived from satellite
63 altimetry (Treichler et al., 2019) and the water balance from hydrological models (Zhou et al.,
64 2015), where the majority of these studies are confined to the Tibetan Plateau (Jiang et al.,
65 2017; G Zhang et al., 2017b).

66 Long-term, regionally consistent time series of lake level datasets and comprehensive
67 assessments of spatiotemporal variations across HMA remained scarce. Satellite altimetry
68 provides an indispensable opportunity for dynamic monitoring of water level changes in lakes



69 over large regions. We use satellite altimetry from CryoSat-2 (2010 to 2023) and ICESat-2
70 (2018 to 2024) to examine water levels changes of 232 lakes across HMA (Fig. 1). We analyse
71 the temporal and spatial characteristics of water level changes, for lakes in both glaciated and
72 non-glaciated catchments, including endorheic lakes. We assessed the regional difference in
73 lake level trends with catchment-scale climate forcing from ERA5-Land across HMA. By
74 integrating multi-mission altimetry with climate reanalysis data across diverse climate settings,
75 we provide new insights into the evolving lake water level changes and spatial heterogeneity.
76 We selected lakes with surface area larger than 20 km² to ensure reliable water level retrievals
77 from both CryoSat-2 and ICESat-2. Smaller lakes, particularly glacial lakes, in high-relief
78 terrain fall below the effective spatial resolution to adequately retrieve the signal; their narrow
79 open water surfaces are highly susceptible to land contamination and off-nadir reflections that
80 degrade the data quality (Jiang et al., 2017; Kleinherenbrink et al., 2015).



81 **Figure 1** Spatial and temporal pattern of lake water level changes in High Mountain Asia. Each
82 circle represents a lake, color shows the trend in lake water level from CryoSat-2 (2010 to
83 2023), corresponding to the colorbar, and the circle size is scaled by area of each lake. (A to J)
84 Water level timeseries of selected lakes, black line for CryoSat-2 (2010-2023) and brown line
85 represent lake level estimates from ICESat-2 (2018-2024). Y-axis of each subplot is water level
86 in meters (EGS).

87 2. Materials and Methods

88 2.1. Lake Water Level based on CryoSat-2 (2010-2023)

89 We examine the variations in water levels of 232 lakes across HMA from 2010 to 2023 using
90 satellite altimetry data from CryoSat-2. We analyse the characteristics of water level changes,



91 including trends and inter-annual variability, for lakes in both glaciated and non-glaciated
92 catchments. More specifically, we use the Level 1b product from the Baseline E Ice Processor
93 (ESA, 2023, 2019a, b) [ftp://science-](ftp://science-pds.cryosat.esa.int/https://earth.esa.int/eogateway/catalog/cryosat-products)
94 [pds.cryosat.esa.int/https://earth.esa.int/eogateway/catalog/cryosat-products](https://earth.esa.int/eogateway/catalog/cryosat-products). To retrieve range
95 estimates, the waveforms are retracked with the Narrow Primary Peak Threshold retracker
96 (Villadsen et al., 2015). The satellite altimetry-based water level with respect to a reference,
97 here the geoid, is derived based on the expression:

$$98 \quad H = h - (R + corr) - N$$

99 Here h is the altitude of the satellite with respect the reference ellipsoid (WGS84), R is the
100 retracked range, or the distance from the satellite to the surface, $corr$ includes corrections for
101 the wet and dry troposphere, ionosphere, pole tide, solid earth tide, and loading tide, and N is
102 the geoid elevation (EGM2008, (Pavlis et al., 2012))

103 Lake specific altimetry footprints are extracted using the SWOT Prior Lake Database (PLD)
104 (Sheng et al., 2016), which includes a global lake boundaries. In addition, we use the Global
105 Surface Water Occurrence raster product by (Pekel et al., 2016). This raster product with 30 m
106 spatial resolution contains the probability, provided as a percentage, of water being present
107 between 1984-2021. Here, we only retain observations if the occurrence value is 75 % or larger.

108 The water level time series is reconstructed via the method presented in Nielsen et al. (2015).
109 In summary, the model includes a random walk as the process part to account for the temporal
110 correlation, and the observations are assumed to follow a mixture between the Normal and
111 Cauchy distributions to ensure robustness of the water level estimates. The Cauchy distribution
112 is characterized by heavier tails compared to the Normal distribution. In contrast to assuming
113 that the observations only follow a normal distribution, the mixture distribution reduces the
114 influence of extreme observations on the estimated mean.

115 To evaluate how measurement uncertainty affects long-term change detection, the posterior
116 water-level variance is carried forward to the trend analysis, where trend uncertainty is
117 quantified using the bootstrap-based Sen's slope procedure described in Section 2.3. The
118 resulting trend uncertainties therefore reflect both measurement noise and temporal sampling
119 variability in the altimetry record. In Nielsen et al (2015) the standard deviation to each
120 estimated mean water level in the timeseries is derived from the generalized delta method
121 (Thorson and Kristensen, 2024) with the main contribution from the Hessian matrix related to
122 the mean water levels and additionally how uncertainty in the fixed model parameters affects



123 these estimates. In the estimation of the mean water levels, correlation among along-track water
124 levels was not accounted for which implies that the standard deviation is underestimated.

125 **2.2. Lake Water Level based on ICESat-2 (2018-2024)**

126 To retrieve the water level time series using ICESat-2 we apply the inland water product
127 ATL13 (Jasinski et al., 2023) version 6. For consistency across mission, ICESat-2 water levels
128 are processed using the same extraction and filtering approach as described above for the
129 CryoSat-2 data. The water level time series are reconstructed at monthly time steps using the
130 methodology described in Nielsen et al., (2015) with the exception that the process part of the
131 state-space model is an autoregressive model of order 1.

132 **2.3. Lake Water Level Trend analysis**

133 To quantify changes in the lake water levels, we analysed trends separately for the CryoSat-2
134 (2010-2023) and ICESat-2 (2018-2024) periods. For the trend analysis we excluded lakes
135 where water levels are regulated. To isolate the signal from intra-annual seasonal fluctuation
136 such as monsoon induced cycles in the central Himalaya, we applied Seasonal-Trend
137 decomposition using LOESS (STL) to the monthly timeseries (Cleveland et al., 1990). STL
138 separates the signal into three components, trend (T), seasonal (S), and residuals \mathbb{R} . The trend
139 captures the low frequency variability, the seasonal components represent periodic cycles, and
140 residuals account for high-frequency variability. For subsequent analysis, we used the de-
141 seasonalized timeseries (T+R) to ensure that estimated trends represent sustained hydrological
142 changes rather than seasonal cycles.

143 We assessed the statistical significance of monotonic trends in the de-seasonalized timeseries
144 using the Mann-Kendall (MK) test ($p < 0.05$), while the magnitude of change was estimated
145 with Sen's slope estimator. Uncertainty in the Sen's slope for each lake is derived from
146 bootstrap resampling ($n = 100$), where the timeseries is resampled with replacement and Sen's
147 slope recalculated. The standard deviation of the resulting slope distribution is taken as the
148 standard error of the trend estimate.

149 We first estimated the trend for individual lakes and then aggregated into subregions based on
150 geographic region (Tibetan Plateau, Himalaya, western High Mountain Asia and lakes in
151 glaciated catchments). Regional trends are calculated as the uncertainty-weighted mean of the
152 individual lake slopes, with the standard error of this weighted mean reported as the uncertainty
153 of the regional trend. This allowed to better constrain the regional trend with lakes with low
154 uncertainty in trend estimates. For comparison we also provided a median lake level change



155 rate. To derive a continuous long-term trend from both altimetry missions, we corrected for
156 systematic offsets between ICESat-2 and CryoSat-2 mainly related to different vertical
157 references in the two missions. Our intercomparison analysis during the overlapping period
158 (2018-2023) shows a systematic bias of +2.74 m between ICESat-2 and CryoSat-2
159 measurements. This offset is consistently observed across 77% of lakes (183 of 238) with
160 statistical significance ($p < 0.05$). We therefore applied a -2.74 m correction to ICESat-2
161 timeseries for the mission intercomparison.

162 **2.4. Climate data analysis**

163 We analysed climate variability across High Mountain Asia using the ERA5-Land reanalysis
164 data (Muñoz Sabater, 2021), We used near-surface air temperature (2 m), total precipitation,
165 and total evaporation for the period of 2010 to 2024, focusing on temporal and spatial
166 variability and trends on annual and seasonal scale. To isolate long-term changes, seasonal
167 cycles were removed by subtracting the monthly climatology (1980–2023) from each series.
168 We analysed trends in de-seasonalized anomalies using the MK test (Mann, 1945; Kendall,
169 1975). Trend magnitudes were estimated using ordinary least squares linear regression,
170 expressed as rate of change per year. Significance in trends is evaluated at 95% confidence
171 level ($p < 0.05$).

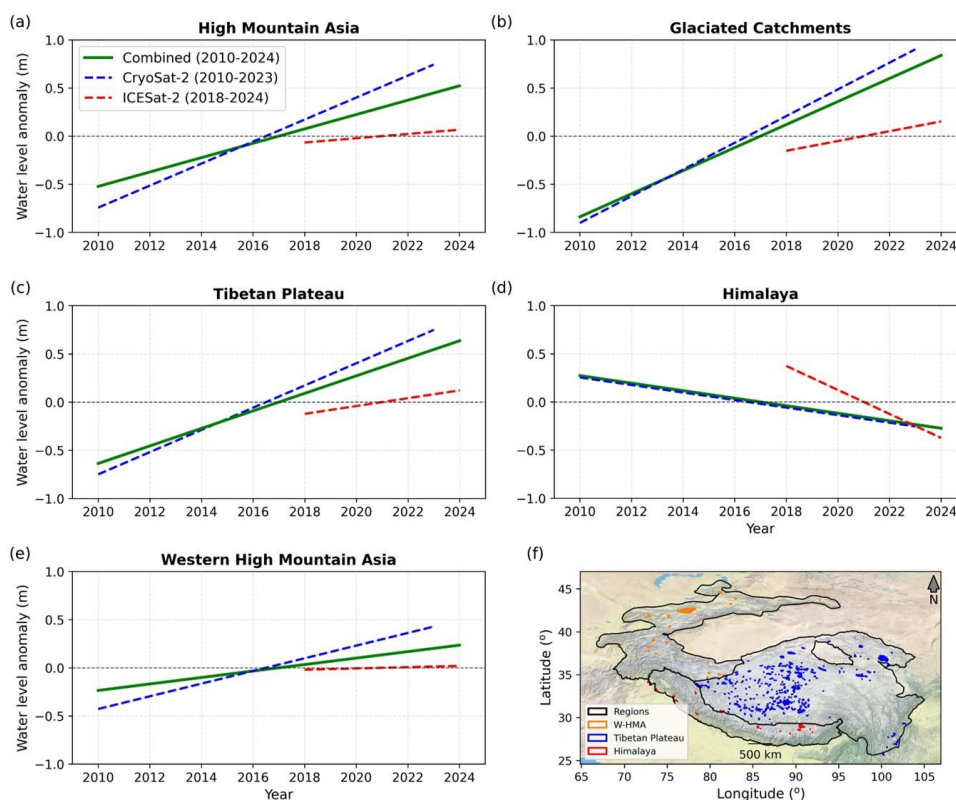
172 We used different methods to remove seasonality in lake water level and climate timeseries.
173 The irregular sampling and string inter-annual cycles complicate the signal for lake water level
174 derived from altimetry, the STL decomposition provides a flexible and robust method for
175 separating trend, seasonality and noise. Climate data from ERA5-Land is regularly sampled
176 and exhibit well-defined seasonal cycles in temperature, precipitation and evaporation
177 therefore, subtracting monthly climatology can effectively remove seasonality, preserving the
178 long-term trend.



179 **3. Results**

180 **3.1. Increasing lake water levels across High Mountain Asia**

181 Our analysis of 232 lakes across HMA reveals a pattern of overall water level increase from
 182 2010 to 2024 with 91% statistically significant trends ($p < 0.05$). The majority of the lakes
 183 analyzed (179, 77%) experience positive water level trend, while 54 lakes (23%) show
 184 declining water levels (Table S1). The median increase in water level is 0.10 m yr^{-1} across all
 185 lakes and 117 lakes (50.4%) experiencing strong increases exceeding 0.1 m yr^{-1} . The
 186 distribution of trend shows considerable variability ($\sigma = 0.23 \text{ m yr}^{-1}$), ranging from rapid
 187 decline (-0.52 m yr^{-1}) to substantial growth ($+1.08 \text{ m yr}^{-1}$). This heterogeneity is further evident
 188 by the interquartile range (0.006 to 0.29 m yr^{-1}), indicating that while most lakes in the region
 189 experienced heightened water levels, the rates varied substantially across HMA. Lake size
 190 exhibited a positive relationship with growth rates, as larger lakes generally showed higher
 191 mean trends (20-100 km^2 : 0.12 m yr^{-1} ; 1000-1000 km^2 : 0.145 m yr^{-1} ; larger than 1000 km^2 :
 192 0.176 m yr^{-1}). Lakes located in higher elevation show more positive trends compared to the
 193 lakes located in lower elevations with a positive correlation between elevation and water level
 194 increase rate ($r = 0.35$).





195 **Figure 2** (a) Regional water level trends across HMA derived from CryoSat-2 (blue, 2010–
196 2023), ICESat-2 (red, 2018–2024), and the combined record after bias correction (green, 2010–
197 2024), (b) lakes within glaciated catchments, (c) Tibetan Plateau, (d) Himalaya, and (e)
198 Western HMA. Shading shows $1-\sigma$ uncertainty. (f) Distribution of lakes highlighted with
199 different color, regions are highlighted with black line.

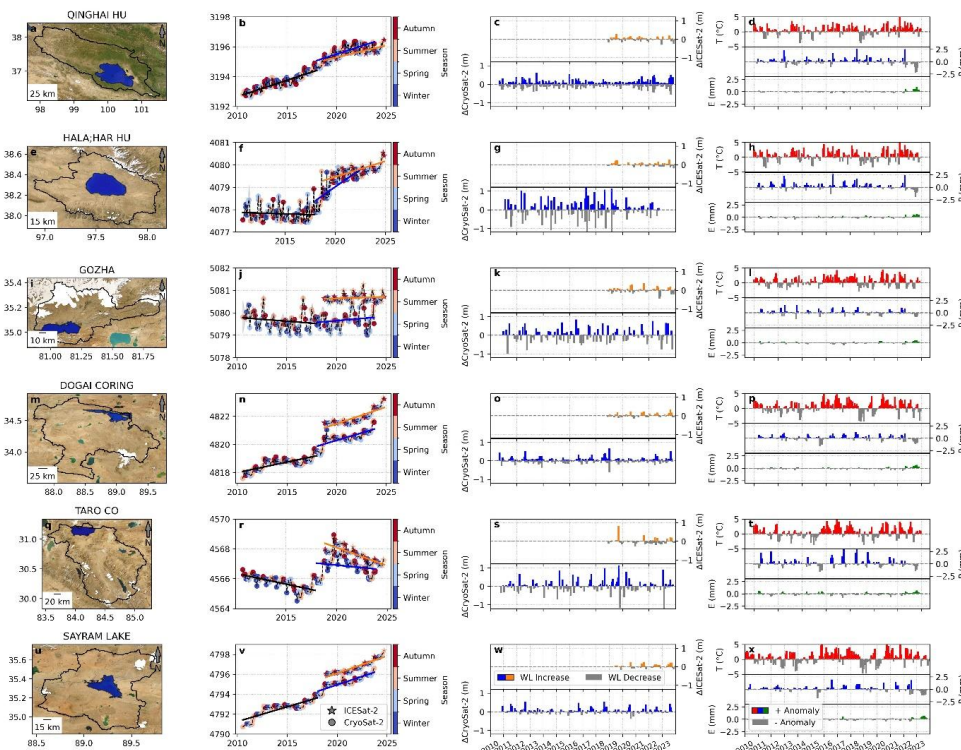
200 During the mission overlap period (2018 to 2023), intercomparison trend shows strong
201 consistency between CryoSat-2 and ICESat-2 with near zero mean bias (-0.0001 ± 0.6177 m)
202 and a precision of 0.37 m (Standard deviation of differences) (Fig. S1). Overall, 64% of lakes
203 exhibit correlation ($r > 0.5$), with 45% particularly strong agreement ($r > 0.7$) (Fig. S1a). Trend
204 estimates from both missions agree for the majority of lakes (80%), indicating consistency
205 between the two sensors. During the CryoSat-2 period (2010 to 2023), lake level increased at
206 a mean rate of 0.15 m yr^{-1} with 117 (49%) experiencing higher rate of increases greater than
207 0.1 m yr^{-1} . However, during the ICESat-2 period (2018 to 2024), the mean increase rate reduced
208 to 0.052 m yr^{-1} with 98 lakes (41%) maintaining a water level increase rate higher than 0.1
209 yr^{-1} . Analysis of trend persistence reveals that 47 lakes that were rising during the early
210 CryoSat-2 period (2010 to 2017) shifted to declining trends in recent years during 2018 to
211 2024, while only 24 lakes transitioned from negative to positive trends.

212 **3.2. Regional variations in lake water level**

213 Lakes on the Tibetan Plateau show a consistent increasing trend across both altimetry periods
214 (2010-2024), with the combined record indicating substantial growth (0.09 ± 0.001 m yr^{-1})
215 (Figure 2c). CryoSat-2 (2010 to 2023) based results show increasing lake levels at a rate of
216 0.18 m yr^{-1} , with 113 lakes (54%) showing consistent increasing trends (>0.1 m yr^{-1}), only 14
217 showed stable water levels (-0.01 to 0.01 m yr^{-1}) and the number of lakes with a strong
218 decreasing trends (<-0.1 m yr^{-1}) is relatively low (7 lakes). The remaining 77 lakes experienced
219 moderate change rates between -0.1 to 0.1 m yr^{-1} . ICESat-2 based results from 2018 to 2024
220 show lower rate of growth (0.004 m yr^{-1}), with only 93 lakes (44%) maintaining strong positive
221 trends (>0.1 m yr^{-1}) and 25 show strong decreasing trends. 26 lakes showed relatively stable
222 trends (-0.01 to 0.01 m yr^{-1}) during 2018 to 2024. We find a modest correlation between lake
223 morphology and water level trends across the Tibetan Plateau. While correlation between the
224 elevation and lake area with trend magnitude are positive but negligible, explaining less than
225 1% of the observed variance. However, we find a clear pattern in lake water level with lake
226 size, larger lakes exhibited systematically higher growth rates, largest lakes (>1000 km²) show
227 higher rate of increasing water levels (0.23 ± 0.18 m yr^{-1}), lakes with an area between 100 to



228 1000 km² shows growth rate of 0.19 ± 0.22 m yr⁻¹ and the lakes with an area between 20 to 100
 229 km² grew by 0.14 ± 19 m yr⁻¹.



230 **Figure 3** Water level change and climate variations from Tibetan Plateau. (a) The Qinghai Hu
 231 Lake is shown in blue and catchment highlighted with black boundary. (b) Water level time
 232 series (m) from CryoSat-2 (2010 – 2023) and ICESat-2 (2018 – 2024). The color corresponds
 233 to the season of data acquisition, correspond to the color bar. The standard deviation of lake
 234 levels is shown in grey. (c) Water level change during CryoSat-2 (blue) and ICESat-2 (yellow).
 235 (d) The colored and grey bars represent anomalies in temperature (T°C), precipitation (P mm)
 236 and Evaporation (E mm). Similarly, for Hala Har Hu Lake, Gozha Lake, Dogai Coring Lake,
 237 Taro Co Lake, and Dogaicoring Qangco Lake in the Tibetan Plateau.

238 In contrast, analyzed lakes in Himalaya region shows persistent decline across both altimetry
 239 datasets (Figure 2d). We find a median decreasing rate of -0.09 m yr⁻¹ during CryoSat-2 (2010
 240 to 2023) and ICESat-2 results show slightly larger declining water levels -0.62 m yr⁻¹ 2018 to
 241 2024. The number of lakes with strong decline (>0.1 m yr⁻¹) increased from the CryoSat-2 (2
 242 lakes; 2018-2023) to ICESat-2 period (4 lakes; 2018-2024). Lake level time series for the lakes
 243 in Himalayan region from both altimeter datasets are presented in Figure S4. Lakes with an
 244 area between 20 to 100 km² are more rapidly decreasing (-0.08 ± 0.15 m yr⁻¹) compared to



245 larger lakes ($-0.03 \pm 0.04 \text{ m yr}^{-1}$). We observed a positive correlation between elevation and
246 trend magnitude ($r = 0.38$).

247 The lakes studied in western HMA, 7 out of 12 lakes experienced consistent growth in lake
248 water level with a mean rate of 0.13 m yr^{-1} during 2010 to 2023 based on CryoSat-2. ICESat-
249 2 results show the slowdown in water levels rise in recent years (2018 to 2024), with growth
250 rate decreasing to near zero (Fig. 2e). However, three lakes transitioned from negative to
251 positive trends between 2010 to 2017 and 2018 to 2024 (Fig. S5). Similarly, large lakes (100
252 to 1000 km^2) experienced a higher increase in water levels ($0.17 \pm 0.21 \text{ m yr}^{-1}$), while lakes
253 with area range between 20 to 100 km^2 experienced a slight decline ($-0.02 \pm 0.10 \text{ m yr}^{-1}$). We
254 find a positive correlation ($r = 0.48$) between elevation and trend magnitude suggesting lakes
255 located in higher elevations are experiencing enhanced growth.

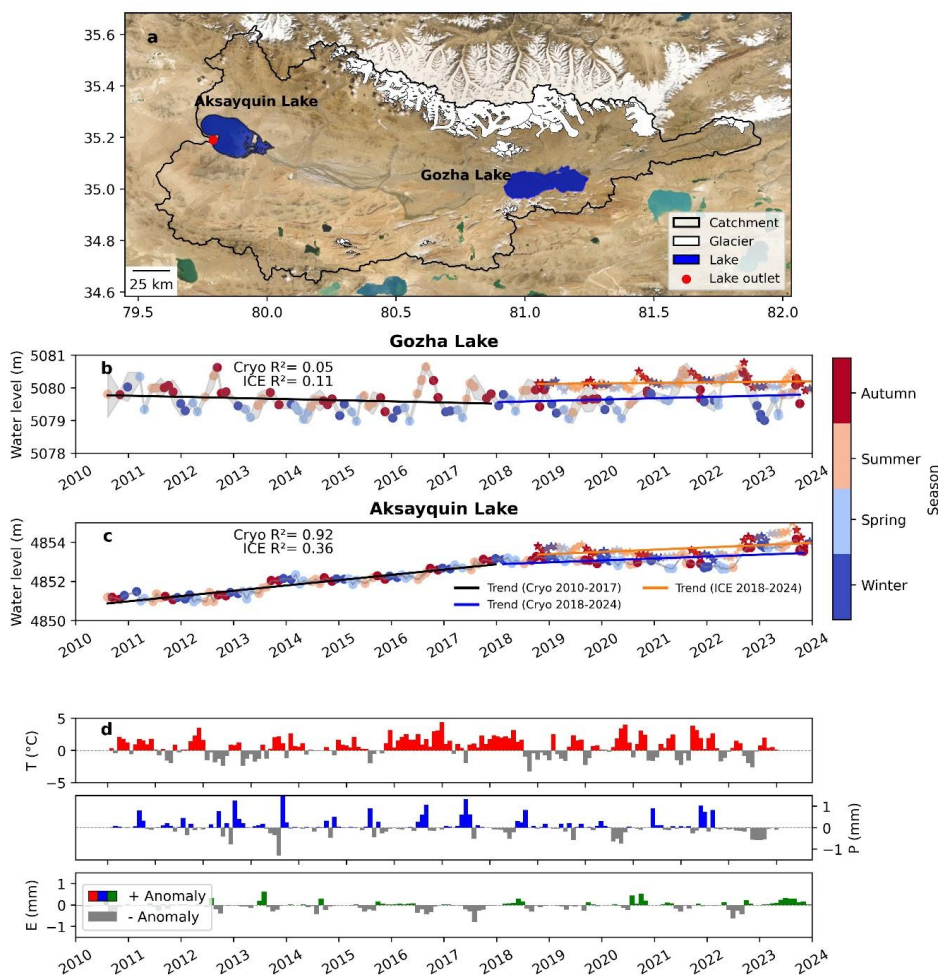
256 Lakes located in the glaciated catchments show an accelerating growth rates based on both
257 altimetry results (2010 to 2023 and 2018 to 2024) with a rate of 0.028 to 0.096 m yr^{-1} ,
258 respectively (Fig. 2b). CryoSat-2 results show that these lakes exhibit highest mean growth rate
259 (0.18 m yr^{-1}) during 2010 to 2023, with 18 out of 37 showing strong increase. ICESat-2 results
260 show the slowdown of rapid increase in water level to 0.016 m yr^{-1} during 2018 to 2024. Lakes
261 within glaciated catchments with an area between 100 to 1000 km^2 maintaining higher rate of
262 increase in water levels ($0.19 \pm 0.27 \text{ m yr}^{-1}$) compared to lakes with an area between 20 to 100
263 km^2 ($0.08 \pm 0.13 \text{ m yr}^{-1}$). We find a slightly weak correlation with elevation ($r = 0.02$) compared
264 to the regional analysis.

265 3.3. Regional Climate trends

266 On Tibetan Plateau, where most lakes are located, correlations with all three climate variables
267 are weak and statistically not significant ($r = 0.09$). Based on seasonal climate data analysis we
268 find that increase in temperature during autumn season is highest across HMA, particularly on
269 the Tibetan Plateau where temperature increased with $+0.15^\circ\text{C yr}^{-1}$, along with $+0.06^\circ\text{C yr}^{-1}$
270 during summer months. Precipitation trends show no statistically significant changes during
271 2010 to 2024. Lakes located in non-glaciated catchments on Tibetan Plateau exhibit a
272 significant positive correlation with precipitation ($r = 0.32$, $p < 0.001$) and a weak negative
273 correlation with evaporation ($r = -0.15$, $p = 0.04$), indicating changes in precipitation play
274 dominant role in water level variability. Large endorheic lakes exhibit sustained water level
275 rise. Qinghai, Hala Har and Sayram Lakes experienced substantial increase with a rate of 0.35
276 $\pm 0.01 \text{ m yr}^{-1}$, $0.43 \pm 0.02 \text{ m yr}^{-1}$, and $0.59 \pm 0.02 \text{ m yr}^{-1}$, respectively during 2010 to 2024.
277 These trends coincide with statistically significant long-term warming ($0.01 \pm 0.002^\circ\text{C yr}^{-1}$ to
278 $0.15 \pm 0.002^\circ\text{C yr}^{-1}$) and slightly increasing precipitation up to $0.02 \pm 0.01 \text{ mm yr}^{-1}$ with no



279 significant long-term evaporation changes (Fig. 2). Similarly, Ayakkum, Achik and Jingyu
 280 Lakes in Eastern Kunlun Shan show rising water levels ($0.54 \pm 0.01 \text{ m yr}^{-1}$, $0.76 \pm 0.02 \text{ m yr}^{-1}$
 281 and $0.75 \pm 0.02 \text{ m yr}^{-1}$, respectively). These three lakes are experiencing a coherent climate
 282 signal of statistically significant increasing temperature ($0.01 \pm 0.002^\circ\text{C yr}^{-1}$) and precipitation
 283 ($0.001 \pm 0.001 \text{ mm yr}^{-1}$) combined with slight reduction in evaporation ($-0.001 \pm 0.00 \text{ mm yr}^{-1}$)
 284 ¹).



285 **Figure 4** (a) The locations of Aksayquin Lake and Gozha Lake situated in the Western Kunlun
 286 Shan region. (b) Water level timeseries of Gozha Lake from CryoSat-2 (2010 to 2023) and
 287 ICESat-2 (2018 to 2024), represented with circle and star, respectively. (c) Similarly, water
 288 level timeseries of Aksayquin Lake from CryoSat-2 and ICESat-2. The color of dot and star in
 289 each timeseries corresponds to the season of data acquisition, indicated by the color bar. The
 290 black and blue lines represent trends from 2010 to 2017 and 2018 to 2023, respectively for the
 291 CryoSat-2 period. The range of error in each time series is shown in gray. (d) Positive



292 anomalies in temperature (T °C), precipitation (P mm) and evaporation (E mm) are shown red,
293 blue and green color, respectively and negative anomalies are in gray.

294 Lake catchments in Himalayan experience an increase in temperature during summer ($+0.06 \pm$
295 $0.01^\circ\text{C yr}^{-1}$) and autumns ($+0.08 \pm 0.04^\circ\text{C yr}^{-1}$) which is statistically significant. Winter
296 precipitation shows a significant decline ($-0.07 \pm 0.03 \text{ mm yr}^{-1}$), while other seasons exhibit
297 weaker, non-significant trends. Lake water level and climate correlations are moderate but non-
298 significant for both temperature ($r = 0.48$) and precipitation ($r = 0.53$), broadly consistent with
299 the declining lake levels. Himalayan lakes, (though few observed, 11), show positive
300 correlations with both temperature and precipitation ($r = 0.48$ and $r = 0.53$, respectively),
301 though neither is statistically significant. Lake catchments across Western HMA show a
302 statistically significant increase in temperature during summer months ($-0.07 \pm 0.04 \text{ mm yr}^{-1}$),
303 with weaker but consistent positive trends in other seasons. Winter and autumn precipitation
304 slightly reduced (-0.05 - and -0.03 - mm yr^{-1}), whereas other seasons do not exhibit strong trends.
305 At the lake catchment scale, western HMA shows a clearer climate signal with precipitation
306 significantly correlated with lake level trends ($r = 0.72$, $p = 0.004$), indicating that modest
307 changes in moisture availability can strongly influence water level.

308 Across HMA lakes within glaciated catchments shows statistically significant increasing
309 temperature trends ($0.06 \pm 0.02^\circ\text{C yr}^{-1}$) with no significant correlation with annual temperature,
310 precipitation and evaporation trends ($r < 0.17$). Despite temperature being the dominant but
311 statistically non-significant predictor among the three variables. This weak climate correlation
312 with lake water level contrasts with the behavior of lower elevation, non-glaciated lakes, where
313 precipitation exerts a stronger influence. The absence of robust correlations in glaciated
314 catchments indicates that interannual water level variability in lakes is strongly influenced by
315 snow and ice melt, including nonlinear melt runoff relationships and hydrological delays, rather
316 than contemporaneous year-to-year climate anomalies. This pattern is clearly visible in lakes
317 such as Aksayquin Lake (4844 m a.s.l.) and the upstream Gozha Lake (5080 m a.s.l.) in
318 Western Kunlun Shan, experienced rising water level trends of $0.21 \pm 0.01 \text{ m yr}^{-1}$ and $0.01 \pm$
319 0.01 m yr^{-1} , respectively during CryoSat-2 period (2010 to 2023) (Fig. 4). Their catchment
320 shows an increasing temperature ($0.05 \pm 0.02^\circ\text{C yr}^{-1}$) with declining precipitation (-0.01 ± 0.01
321 to $-0.02 \pm 0.01 \text{ mm yr}^{-1}$) and negligible long-term changes in evaporation. Despite these long-
322 term lake level increase, annual correlation with climate variables remained weak ($r < 0.15$).
323 Gozha lake shows significant negative winter precipitation correlation ($r = -0.44$, $p < 0.05$) and
324 a weak positive autumn temperature correlation ($r = 0.33$, $p < 0.05$), suggesting snow
325 accumulation delays meltwater runoff. Similarly, Burog Co and Niri Acuogai Lakes on Tibetan
326 Plateau shows increasing water levels by $0.54 \pm 0.04 \text{ m yr}^{-1}$ and $0.26 \pm 0.02 \text{ m yr}^{-1}$, respectively



327 (Fig. S3). Both catchments exhibit sustained increasing temperatures, $0.07 \pm 0.03^\circ\text{C yr}^{-1}$ at
 328 Burog Co and a higher rate of $0.17 \pm 0.04^\circ\text{C yr}^{-1}$ at Niri Acuogai Lake, while precipitation
 329 trends remain negative, and evaporation trends minimal (Fig. S3). These differences are
 330 consistent with their (Gozha and Burog Co Lakes) hydrological positions adjacent to glacier
 331 and predominantly reflect immediate meltwater inputs, whereas Aksayquin and Niri Acuogai
 332 Lakes integrate both local melt and inflows routed from wider catchment upstream.

333 **Table 1** Regional trends in lake water level (m yr^{-1}) across High Mountain Asia. Uncertainty
 334 weighted mean of individual lakes within three median absolute deviations. The combined
 335 trend represents the period 2010-2024. Lakes with water levels regulated by human activities
 336 are excluded for regional trend analysis.

Region	Altimetry mission	Period	Trend (m yr^{-1})	Number of lakes analyzed
High Mountain Asia	CryoSat-2	2010-2017	0.036 ± 0.001	194/232
	CryoSat-2	2018-2023	-0.055 ± 0.001	203/232
	ICESat-2	2018-2024	0.022 ± 0.002	209/232
	Combined	2010-2024	0.07 ± 0.001	202/232
Glaciated Catchments	CryoSat-2	2010-2017	0.028 ± 0.004	34/37
	CryoSat-2	2018-2023	0.096 ± 0.006	32/37
	ICESat-2	2018-2024	0.051 ± 0.007	36/37
	Combined	2010-2024	0.065 ± 0.002	33/37
Tibetan Plateau	CryoSat-2	2010-2017	0.041 ± 0.002	174/211
	CryoSat-2	2018-2023	0.120 ± 0.002	184/211
	ICESat-2	2018-2024	0.041 ± 0.002	185/211
	Combined	2010-2024	0.091 ± 0.001	181/211
Himalaya	CryoSat-2	2010-2017	-0.071 ± 0.009	9/9
	CryoSat-2	2018-2023	-0.095 ± 0.013	9/9
	ICESat-2	2018-2024	-0.125 ± 0.007	9/9
	Combined	2010-2024	-0.039 ± 0.003	9/9
Western HMA	CryoSat-2	2010-2017	0.101 ± 0.006	11/12
	CryoSat-2	2018-2023	0.010 ± 0.008	8/12
	ICESat-2	2018-2024	0.005 ± 0.006	7/12



Combined	2010-2024	0.034 ± 0.002	8/12
----------	-----------	-------------------	------

337 **4. Discussion**

338 Our analysis of 232 lakes across HMA reveals a complex and heterogeneous pattern of lake
339 water level change from 2010 to 2024, characterized by widespread but regionally divergent
340 trends. The observed overall increase, with 77% of lakes rising at a median rate of 0.10 m yr^{-1} ,
341 (Table S1) aligns with the well documented lake expansion on the Tibetan Plateau since the
342 early 2000s (Lei et al., 2022; Lei et al., 2014; Zhang et al., 2019). However, our extended record
343 through 2024 and subregional analysis provides new insights into the evolving hydrological
344 drivers and the fate of the notable 2016-2018 precipitation anomaly (Lei et al., 2019). The
345 strong inter-mission consistency (80% sign agreement, $p = 0.013$) between CryoSat-2 and
346 ICESat-2 during 2018-2023 overlap period underscores the robustness of these findings,
347 despite a systematic $+2.74 \text{ m}$ bias stemming mainly from differences in use of quasi-geoid
348 based on EGM2008 for CryoSat-2 and EGM2008 geoid model to ICESat-2. The statistical
349 summary of water level changes for each lake is presented in Table S3 (Supplementary Data).

350 The Tibetan Plateau remains the primary contributor to regional lake water level increase
351 during 2010 to 2024 (Table 1). This rising water level trends are particularly pronounced in the
352 northern and Inner Tibetan Plateau, consistent with previous studies attributing expansion to
353 spatially variable precipitation regimes (Jiang et al., 2023; Kuang and Jiao, 2016). Our
354 catchment-scale analysis shows precipitation variability as the dominant driver of de-seasoned
355 lake trends, with a significant positive correlation ($r = 0.42$, $p < 0.001$) except for lakes within
356 glaciated systems such as endorheic basins in Tibetan Plateau (Jiang et al., 2020; Zhang et al.,
357 2017a; Zhang et al., 2017b). When compared with individual lake water level time series
358 derived from satellite altimetry and in situ measurements, our estimates show strong agreement
359 with previous studies (Lei et al., 2022; Zhang et al., 2019; Zhang et al., 2017b). For the 57
360 lakes common to Zhang et al. (2019), we estimate a mean water level increase of 0.20 ± 0.04
361 m yr^{-1} during 2010 to 2018 (CryoSat-2), which is lower compared to $0.28 \pm 0.03 \text{ m yr}^{-1}$ for
362 2003 to 2018 based on ICESat and ICESat-2. This difference in the mean trend is primarily
363 driven by Seling Co, Wulanwula Lake, and Meiriqie Co, which exhibit the largest
364 discrepancies, with differences range between -0.29 ± 0.01 to $-0.25 \pm 0.02 \text{ m yr}^{-1}$. For lakes
365 with declining water levels, our CryoSat-2 based estimates for 2010 to 2018 closely match
366 those of Zhang et al. (2019) (Table S2), with the exception of Namuka Co, where our estimated
367 rate of decrease is $0.15 \pm 0.03 \text{ m yr}^{-1}$ higher. The persistence of elevated levels in many lakes
368 following the 2016-2018 wet anomaly (Lei et al., 2019) suggests that this episodic pulse had



369 lasting impacts on regional lake hydrology, though its effect was mediated by catchment
370 properties such as storage capacity and groundwater connectivity (Jiang et al., 2020; Lei et al.,
371 2022; Lei et al., 2019). The recent modest deceleration in growth rates observed in the ICESat-
372 2 record (2018-2024) aligns with the sharp precipitation decline in our ERA5-Land analysis
373 post-2021, highlighting the ongoing sensitivity of these systems to interannual precipitation
374 variability (Fig. S2). Lake expansion on Tibetan Plateau in recent decades have been attributed
375 to precipitation, evaporation (Biskop et al., 2016; Yang et al., 2017), Snow and ice melt (Zhang
376 et al., 2017b) ground Water (Lei et al., 2022). Climate data from meteorological station on
377 Plateau shows increasing precipitation trend during 1978 to 2013, except for few stations on
378 southeast Tibetan Plateau (Zhang et al., 2017a) consistent with lake water level changes (Fig.
379 2).

380 Lakes in glaciated catchments shows rising trends in water level. Despite significant regional
381 warming ($0.06 \pm 0.02^{\circ}\text{C yr}^{-1}$), these lakes exhibit weak and statistically non-significant
382 correlations with annual temperature, precipitation, and evaporation ($r < 0.17$). This apparent
383 decoupling from contemporaneous climate anomalies, observed in rapidly rising lakes
384 highlights the dominance of nonlinear cryosphere processes. The significant negative
385 correlation between winter precipitation and Gozha Lake levels ($r = -0.44$, $p < 0.05$) suggests
386 snow accumulation delays meltwater runoff, while weak positive autumn temperature
387 correlations ($r = 0.33$, $p < 0.05$) indicate thermal controls on melt timing. This cryospheric
388 buffering effect, where glacier and snow melt mediate the relationship between climate forcing
389 and lake response, creates a complex hydrological regime that contrasts sharply with
390 precipitation dominated catchments (Yao et al., 2022). High-frequency observations from
391 glacier-fed Blue Moon Lake Valley in southeastern Tibetan Plateau shows glacier melt as a
392 dominant driver of water level changes (5.2 m per unit melt increase, $p < 10^{-176}$) exceeding the
393 modest effect of rainfall (0.47 m, $p = 0.03$) with a meltwater transit time of about 4 hours from
394 glacier to lake (Ai et al., 2024). Such temporal decoupling between melt and lake water level
395 response exemplifies the cryosphere buffering in lakes near glaciers and weak direct correlation
396 with instantaneous climate variables. Increasing lake water levels in endorheic basin during
397 2003-2009 on the Tibetan Plateau has been attributed to increasing precipitation (74%),
398 accelerated glacier melt (13%), and permafrost degradation (12%) (Zhang et al., 2017b), while
399 the processes responsible are yet to be investigated to close the lake water budget across HMA.
400 Lake-catchment scale studies shows that cryosphere meltwater plays an important role in lake
401 water budget Zhang et al. (2024) attributed 62.5% of the increase in Dogai Coring lake storage
402 to glacier mass loss and 19.3% of the lake volume increase to permafrost degradation during
403 2014-2020. Ground ice melt contribution to the Selin Co lake volume expansion is estimated



404 to be 12% during 2017-2020 (Wang et al., 2022). These permafrost contributions are consistent
405 with boreholes observation on the Tibetan Plateau showing that the active layer thickened at
406 an average rate of 19.5 cm/decade with an acceleration in recent years during 1981 to 2018
407 (Zhao et al., 2020). The accelerating growth rates in glaciated catchments from CryoSat-2
408 (0.028 m yr^{-1}) to ICESat-2 (0.096 m yr^{-1}) periods may reflect enhanced meltwater contributions
409 under sustained warming, consistent with glacier mass loss across HMA (Hugonnet et al.,
410 2021; Zemp et al., 2025).

411 In contrast to the Tibetan Plateau, Himalayan lakes show persistent decline, with a median rate
412 of -0.09 m yr^{-1} (CryoSat-2) intensifying to -0.62 m yr^{-1} (ICESat-2). This pattern aligns with
413 observed precipitation decreases and warming in the region (Salerno et al., 2025). Zhang et al.
414 (2017a) estimated decreasing lake area in the Brahmaputra basin since 1998 attributed to
415 decreased precipitation. The inverse size relationship in the Himalaya, where smaller lakes (20-
416 100 km^2) decline more rapidly ($-0.08 \pm 0.15 \text{ m yr}^{-1}$) than larger counterparts ($-0.03 \pm 0.04 \text{ m}$
417 yr^{-1}), suggests limited hydrological resilience in smaller catchments. Combined with shorter
418 residence times and reduced capacity for cryosphere melt buffering, these systems appear
419 highly vulnerable to precipitation deficits (Khanal et al., 2021; Treichler et al., 2019). Western
420 HMA presents an intermediate case, where precipitation emerges as a significant correlate ($r =$
421 0.72 , $p = 0.004$) despite overall mixed trends, indicating a transition zone between precipitation
422 dominated and cryosphere influenced regimes.

423 The systematic relationship between lake area and growth rates across most regions, with the
424 largest lakes ($>1000 \text{ km}^2$) showing the most rapid increases, suggests that larger water bodies
425 integrate runoff from more extensive catchments and exhibit greater resilience to interannual
426 variability. This pattern was particularly evident on the Tibetan Plateau align with the finding
427 of Zhang et al. (2019), though the statistical correlations were weak ($r = 0.09$), indicating that
428 other catchment properties modulate this relationship such as precipitation. The difference
429 between median individual lake trends ($+0.10 \text{ m yr}^{-1}$) and uncertainty-weighted regional means
430 ($+0.07 \pm 0.01 \text{ m yr}^{-1}$) likely reflects the higher measurement uncertainties in smaller lakes (Fig.
431 S1), though it may also indicate slightly different change rates across the lake size spectrum.
432 In altimetry, geoid errors, winter lake ice contamination, and retracking biases present potential
433 limitations (Jiang et al., 2019; Meloni et al., 2020), though these predominantly affect annual
434 signal interpretation rather than the long-term trends analyzed here. While ERA5-Land
435 provides consistent spatiotemporal coverage, its performance in high elevations with complex
436 topography remains uncertain due to coarse resolution and sparse ground observations
437 (Orsolini et al., 2019; Tazi et al., 2024). Consequently, absolute magnitudes of precipitation



438 and evaporation trends should be interpreted cautiously, though relative variability is generally
439 reliable.

440 The heterogeneous lake responses documented in this study have important implications for
441 water resources and hazards across HMA. Water level increase in endorheic lakes enhances
442 surface water availability, while basins reliant on dominant glacier melt contributions face an
443 uncertain trajectory as transient melt subsidies eventually with continued glacier retreat
444 (Hassan et al., 2026; Hugonnet et al., 2021). The rapid growth of proglacial lakes (Chen et al.,
445 2021), combined with an increasing population and infrastructure in downstream areas,
446 heightens GLOF risks for vulnerable communities (Shugar et al., 2020; Taylor et al., 2023).
447 Our observed increase in lakes with strong decline in the Himalaya underscores hydrological
448 vulnerability of these lakes. By providing consistent, multi-mission lake-level trends from
449 CryoSat-2 (2010 – 2023) and ICESat-2 (2018 – 2024), this study improves the temporal
450 continuity and robustness of altimetry-based lake monitoring in HMA. These findings establish
451 a valuable observational baseline for future assessments of regional hydrological change and
452 climate-driven impacts on alpine water resources.

453 **5. Conclusion**

454 This study presents a comprehensive analysis of lake level changes across HMA from 2010 to
455 2024, leveraging timeseries derived based on CryoSat-2 and ICESat-2. Our results show
456 regionally heterogeneous pattern, dominated by increasing trends on the Tibetan Plateau and
457 declining water levels in Himalaya. The robust agreement between the CryoSat-2 and ICESat-
458 2 observations during the overlapping period (2018-2023) confirms the reliability of these
459 trends. The persistence of lake level increase on the Tibetan Plateau through 2024,
460 demonstrates the extended hydrological impact of the 2016-2018 precipitation anomaly,
461 though some lakes experienced declining lake levels in recent years. The divergent response of
462 Himalayan lakes, with accelerating declines, particularly smaller lakes highlights the
463 heightened vulnerability of precipitation changes and reduced cryosphere melt buffering
464 capacity. The stronger increasing water level trends of lakes within glaciated catchments with
465 overall weak and inconsistent correlations with contemporary climate variables highlight the
466 dominant role of nonlinear glacio-hydrology processes and hydrological buffering in mediating
467 response to climate change. The systematic relationship between lakes size, elevation and
468 water level rates proved valuable insights for understanding differential vulnerability across
469 the region. The consistent pattern of larger lakes exhibiting higher rate of increasing lake level
470 suggest greater hydrological resilience to integrate runoff from extensive catchments, while the



471 inverse size relationship in Himalaya points to the vulnerability of smaller lakes in declining
472 precipitation regimes. The climate-change exposure represented by 250 million people
473 dependent on HMA runoff presents (Immerzeel et al., 2020; Pritchard, 2019) a strong impetus
474 to improve our understanding of the lake water level variability across HMA. The regionally
475 heterogeneous response with accelerating water levels in heavily glacierized catchments and
476 declining water levels in precipitation sensitive regions demand tailored adaptation strategies.
477 The integration of multi-mission altimetry with climate reanalysis data provides an important
478 approach for continuous monitoring of these changes and informs water resource management.

479 **Data Availability**

480 The CryoSat-2 data are available at: (ESA, 2023, 2019a, b). The HMA lake boundary file is
481 available as a data Supplement to this publication. High Mountain Asia subregion boundaries
482 are also available at: (Bolch et al., 2019). Lake water level timeseries from this study will be
483 made available through GEUS Bulletin (<https://geusbulletin.org/index.php/geusb>).

484 **Supplement**

485 Supplementary information for this paper is available in the Supplement

486 **Author contributions**

487 JH, KN, and SAK conceptualized and designed the study and methodology, processed data,
488 visualization, and drafted the manuscript with contributions from all co-authors. KN performed
489 simulations for processing altimetry data. WC, RBK, MK, and SAK contributed to
490 conceptualization, interpretation, discussion, review, and editing.

491 **Competing interests**

492 All other authors declare they have no competing interests.

493 **Acknowledgements**

494 Authors acknowledge support from the CryoSat-2 and ICESat-2 Project to make the data freely
495 available for this research. We thank the editor and reviewers for taking time to review and
496 comment on the manuscript.



497 References

- 498 Ai, S., Shah, S. A., Cai, Y., Ling, J., Chu, X., Wang, S., Yang, Y., Ouyang, R., An, J., and
499 Rack, W.: Lake pulses driven by glacier melting and climate variability, *Scientific Reports*, 14,
500 31623, <https://doi.org/10.1038/s41598-024-78660-4>, 2024.
- 501 Biskop, S., Maussion, F., Krause, P., and Fink, M.: Differences in the water-balance
502 components of four lakes in the southern-central Tibetan Plateau, *Hydrol. Earth Syst. Sci.*, 20,
503 209-225, <https://doi.org/10.5194/hess-20-209-2016>, 2016.
- 504 Bolch, T., Shea, J. M., Liu, S., Azam, F. M., Gao, Y., Gruber, S., Immerzeel, W. W., Kulkarni,
505 A., Li, H., Tahir, A. A., Zhang, G., and Zhang, Y.: Status and Change of the Cryosphere in the
506 Extended Hindu Kush Himalaya Region. In: *The Hindu Kush Himalaya Assessment: Mountains, Climate Change, Sustainability and People*, Wester, P., Mishra, A., Mukherji, A.,
507 and Shrestha, A. B. (Eds.), Springer International Publishing, Cham, 10.1007/978-3-319-
508 92288-1_7, 2019.
- 510 Chen, F., Zhang, M., Guo, H., Allen, S., Kargel, J. S., Haritashya, U. K., and Watson, C. S.:
511 Annual 30 m dataset for glacial lakes in High Mountain Asia from 2008 to 2017, *Earth Syst.*
512 *Sci. Data*, 13, 741-766, <https://doi.org/10.5194/essd-13-741-2021>, 2021.
- 513 Cleveland, R. B., Cleveland, W. S., and Terpenning, I.: STL: A Seasonal-Trend Decomposition
514 Procedure Based on Loess, *Journal of Official Statistics*, 6, 3, 1990.
- 515 Duan, A. and Xiao, Z.: Does the climate warming hiatus exist over the Tibetan Plateau?,
516 *Scientific Reports*, 5, 13711, <https://doi.org/10.1038/srep13711>, 2015.
- 517 ESA: European Space Agency L1b LRM Precise Orbit, Baseline E,
518 <https://doi.org/10.5270/CR2-41ad749>, 2023.
- 519 ESA: European Space Agency L1b SARin Precise Orbit Baseline E,
520 <https://doi.org/10.5270/CR2-6afef01>, 2019a.
- 521 ESA: European Space Agency L1b SAR Precise Orbit Baseline E,
522 <https://doi.org/10.5270/CR2-fbae3cd>, 2019b.
- 523 Hassan, J., Colgan, W., Nielsen, K., Kayastha, R. B., Khadka, M., and Khan, S. A.:
524 Accelerating High Mountain Asia Glacier Loss From ICESat and ICESat-2, *IEEE Transactions*
525 *on Geoscience and Remote Sensing*, 64, 1-12, <https://doi.org/10.1109/TGRS.2025.3648542>,
526 2026.
- 527 Hugonnet, R., McNabb, R., Berthier, E., Menounos, B., Nuth, C., Girod, L., Farinotti, D., Huss,
528 M., Dussaillant, I., Brun, F., and Kääb, A.: Accelerated global glacier mass loss in the early
529 twenty-first century, *Nature*, 592, 726-731, <https://doi.org/10.1038/s41586-021-03436-z>,
530 2021.
- 531 Immerzeel, W. W., Lutz, A. F., Andrade, M., Bahl, A., Biemans, H., Bolch, T., Hyde, S.,
532 Brumby, S., Davies, B. J., Elmore, A. C., Emmer, A., Feng, M., Fernández, A., Haritashya, U.,
533 Kargel, J. S., Koppes, M., Kraaijenbrink, P. D. A., Kulkarni, A. V., Mayewski, P. A., Nepal,
534 S., Pacheco, P., Painter, T. H., Pellicciotti, F., Rajaram, H., Rupper, S., Sinisalo, A., Shrestha,
535 A. B., Viviroli, D., Wada, Y., Xiao, C., Yao, T., and Baillie, J. E. M.: Importance and
536 vulnerability of the world's water towers, *Nature*, 577, 364-369, 10.1038/s41586-019-1822-y,
537 2020.
- 538 Jasinski, M., Stoll, J., Hancock, D., Robbins, J., Nattala, J., Pavelsky, T., Morison, J., Jones,
539 B., Ondrusek, M., Parrish, C., Carabajal, C., and Team, T. I.-S.: ATLAS/ICESat-2 L3A Along
540 Track Inland Surface Water Data, Version 6. NASA National Snow and Ice Data Center
541 Distributed Active Archive Center, <https://doi.org/10.5067/ATLAS/ATL13.006>, 2023.
- 542 Jiang, J., Zhou, T., Qian, Y., Li, C., Song, F., Li, H., Chen, X., Zhang, W., and Chen, Z.:
543 Precipitation regime changes in High Mountain Asia driven by cleaner air, *Nature*, 623, 544-
544 549, <https://doi.org/10.1038/s41586-023-06619-y>, 2023.
- 545 Jiang, L., Andersen, O. B., Nielsen, K., Zhang, G., and Bauer-Gottwein, P.: Influence of local
546 geoid variation on water surface elevation estimates derived from multi-mission altimetry for
547 Lake Namco, *Remote Sensing of Environment*, 221, 65-79,
548 <https://doi.org/10.1016/j.rse.2018.11.004>, 2019.



- 549 Jiang, L., Nielsen, K., Andersen, O. B., and Bauer-Gottwein, P.: A Bigger Picture of how the
550 Tibetan Lakes Have Changed Over the Past Decade Revealed by CryoSat-2 Altimetry, *Journal*
551 *of Geophysical Research: Atmospheres*, 125, e2020JD033161,
552 <https://doi.org/10.1029/2020JD033161>, 2020.
- 553 Jiang, L., Nielsen, K., Andersen, O. B., and Bauer-Gottwein, P.: Monitoring recent lake level
554 variations on the Tibetan Plateau using CryoSat-2 SARIn mode data, *Journal of Hydrology*,
555 544, 109-124, <https://doi.org/10.1016/j.jhydrol.2016.11.024>, 2017.
- 556 Khanal, S., Lutz, A. F., Kraaijenbrink, P. D. A., van den Hurk, B., Yao, T., and Immerzeel, W.
557 W.: Variable 21st Century Climate Change Response for Rivers in High Mountain Asia at
558 Seasonal to Decadal Time Scales, *Water Resources Research*, 57, e2020WR029266,
559 <https://doi.org/10.1029/2020WR029266>, 2021.
- 560 Kleinherenbrink, M., Lindenbergh, R. C., and Ditmar, P. G.: Monitoring of lake level changes
561 on the Tibetan Plateau and Tian Shan by retracking Cryosat SARIn waveforms, *Journal of*
562 *Hydrology*, 521, 119-131, <https://doi.org/10.1016/j.jhydrol.2014.11.063>, 2015.
- 563 Kuang, X. and Jiao, J. J.: Review on climate change on the Tibetan Plateau during the last half
564 century, *Journal of Geophysical Research: Atmospheres*, 121, 3979-4007,
565 <https://doi.org/10.1002/2015JD024728>, 2016.
- 566 Lei, Y., Yang, K., Immerzeel, W. W., Song, P., Bird, B. W., He, J., Zhao, H., and Li, Z.: Critical
567 Role of Groundwater Inflow in Sustaining Lake Water Balance on the Western Tibetan Plateau,
568 *Geophysical Research Letters*, 49, e2022GL099268, <https://doi.org/10.1029/2022GL099268>,
569 2022.
- 570 Lei, Y., Yang, K., Wang, B., Sheng, Y., Bird, B. W., Zhang, G., and Tian, L.: Response of
571 inland lake dynamics over the Tibetan Plateau to climate change, *Climatic Change*, 125, 281-
572 290, <https://doi.org/10.1007/s10584-014-1175-3>, 2014.
- 573 Lei, Y., Yao, T., Yang, K., Sheng, Y., Kleinherenbrink, M., Yi, S., Bird, B. W., Zhang, X.,
574 Zhu, L., and Zhang, G.: Lake seasonality across the Tibetan Plateau and their varying
575 relationship with regional mass changes and local hydrology, *Geophysical Research Letters*,
576 44, 892-900, <https://doi.org/10.1002/2016GL072062>, 2017.
- 577 Lei, Y., Zhu, Y., Wang, B., Yao, T., Yang, K., Zhang, X., Zhai, J., and Ma, N.: Extreme Lake
578 Level Changes on the Tibetan Plateau Associated With the 2015/2016 El Niño, *Geophysical*
579 *Research Letters*, 46, 5889-5898, <https://doi.org/10.1029/2019GL081946>, 2019.
- 580 Meloni, M., Bouffard, J., Parrinello, T., Dawson, G., Garnier, F., Helm, V., Di Bella, A.,
581 Hendricks, S., Ricker, R., Webb, E., Wright, B., Nielsen, K., Lee, S., Passaro, M., Scagliola,
582 M., Simonsen, S. B., Sandberg Sørensen, L., Brockley, D., Baker, S., Fleury, S., Bamber, J.,
583 Maestri, L., Skourup, H., Forsberg, R., and Mizzi, L.: CryoSat Ice Baseline-D validation and
584 evolutions, *The Cryosphere*, 14, 1889-1907, <https://doi.org/10.5194/tc-14-1889-2020>, 2020.
- 585 Muhammad, S.: HKH snow update 2024, International Centre for Integrated Mountain
586 Development (ICIMOD), Nepal, <https://doi.org/10.53055/ICIMOD.1046>, 2024.
- 587 Muñoz Sabater, J.: ERA5-Land hourly data from 1950 to present Copernicus Climate Change
588 Service (C3S) Climate Data Store (CDS), <https://doi.org/10.24381/cds.e2161bac>, 2021.
- 589 Na, Y., Lu, R., Fu, Q., and Leung, L. R.: Extreme Precipitation Over the Southern Slope of the
590 Tibetan Plateau and the Associated Atmospheric Circulation Anomalies, *Journal of*
591 *Geophysical Research: Atmospheres*, 129, e2024JD040872,
592 <https://doi.org/10.1029/2024JD040872>, 2024.
- 593 Nielsen, K., Stenseng, L., Andersen, O. B., Villadsen, H., and Knudsen, P.: Validation of
594 CryoSat-2 SAR mode based lake levels, *Remote Sensing of Environment*, 171, 162-170,
595 <https://doi.org/10.1016/j.rse.2015.10.023>, 2015.
- 596 Niu, X., Tang, J., Chen, D., Wang, S., and Ou, T.: Elevation-Dependent Warming Over the
597 Tibetan Plateau From an Ensemble of CORDEX-EA Regional Climate Simulations, *Journal*
598 *of Geophysical Research: Atmospheres*, 126, e2020JD033997,
599 <https://doi.org/10.1029/2020JD033997>, 2021.
- 600 Orsolini, Y., Wegmann, M., Dutra, E., Liu, B., Balsamo, G., Yang, K., de Rosnay, P., Zhu, C.,
601 Wang, W., Senan, R., and Arduini, G.: Evaluation of snow depth and snow cover over the



- 602 Tibetan Plateau in global reanalyses using in situ and satellite remote sensing observations,
603 The Cryosphere, 13, 2221-2239, <https://doi.org/10.5194/tc-13-2221-2019>, 2019.
- 604 Ouyang, L., Yang, K., Lu, H., Chen, Y., Lazhu, Zhou, X., and Wang, Y.: Ground-Based
605 Observations Reveal Unique Valley Precipitation Patterns in the Central Himalaya, Journal of
606 Geophysical Research: Atmospheres, 125, e2019JD031502,
607 <https://doi.org/10.1029/2019JD031502>, 2020.
- 608 Pritchard, H. D.: Asia's shrinking glaciers protect large populations from drought stress,
609 Nature, 569, 649-654, <https://doi.org/10.1038/s41586-019-1240-1>, 2019.
- 610 Salerno, F., Guyennon, N., Colombo, N., Melis, M. T., Dessi, F. G., Verza, G., Bista, K.,
611 Sheharyar, A., and Tartari, G.: What is climate change doing in the Himalaya? Thirty years of
612 the Pyramid Meteorological Network (Nepal), Earth Syst. Sci. Data, 17, 4293-4304,
613 <https://doi.org/10.5194/essd-17-4293-2025>, 2025.
- 614 Shugar, D. H., Burr, A., Haritashya, U. K., Kargel, J. S., Watson, C. S., Kennedy, M. C.,
615 Bevington, A. R., Betts, R. A., Harrison, S., and Stratman, K.: Rapid worldwide growth of
616 glacial lakes since 1990, Nature Climate Change, 10, 939-945, 10.1038/s41558-020-0855-4,
617 2020.
- 618 Song, C. and Sheng, Y.: Contrasting evolution patterns between glacier-fed and non-glacier-
619 fed lakes in the Tanggula Mountains and climate cause analysis, Climatic Change, 135, 493-
620 507, <https://doi.org/10.1007/s10584-015-1578-9>, 2016.
- 621 Taylor, C., Robinson, T. R., Dunning, S., Rachel Carr, J., and Westoby, M.: Glacial lake
622 outburst floods threaten millions globally, Nature Communications, 14, 487, 10.1038/s41467-
623 023-36033-x, 2023.
- 624 Tazi, K., Orr, A., Hernandez-González, J., Hosking, S., and Turner, R. E.: Downscaling
625 precipitation over High-mountain Asia using multi-fidelity Gaussian processes: improved
626 estimates from ERA5, Hydrol. Earth Syst. Sci., 28, 4903-4925, <https://doi.org/10.5194/hess-28-4903-2024>, 2024.
- 628 Thorson, J. and Kristensen, K.: Spatio-Temporal Models for Ecologists. Chapman and
629 Hall/CRC, <https://doi.org/10.1201/9781003410294>, 2024.
- 630 Treichler, D., Kääh, A., Salzmann, N., and Xu, C. Y.: Recent glacier and lake changes in High
631 Mountain Asia and their relation to precipitation changes, The Cryosphere, 13, 2977-3005,
632 <https://doi.org/10.5194/tc-13-2977-2019>, 2019.
- 633 Wang, L., Zhao, L., Zhou, H., Liu, S., Du, E., Zou, D., Liu, G., Xiao, Y., Hu, G., Wang, C.,
634 Sun, Z., Li, Z., Qiao, Y., Wu, T., Li, C., and Li, X.: Contribution of ground ice melting to the
635 expansion of Selin Co (lake) on the Tibetan Plateau, The Cryosphere, 16, 2745-2767,
636 <https://doi.org/10.5194/tc-16-2745-2022>, 2022.
- 637 Wu, F., You, Q., Cai, Z., Sun, G., Normatov, I., and Shrestha, S.: Significant elevation
638 dependent warming over the Tibetan Plateau after removing longitude and latitude factors,
639 Atmospheric Research, 284, 106603, <https://doi.org/10.1016/j.atmosres.2022.106603>, 2023.
- 640 Yang, K., Yao, F., Wang, J., Luo, J., Shen, Z., Wang, C., and Song, C.: Recent dynamics of
641 alpine lakes on the endorheic Changtang Plateau from multi-mission satellite data, Journal of
642 Hydrology, 552, 633-645, <https://doi.org/10.1016/j.jhydrol.2017.07.024>, 2017.
- 643 Yao, T., Bolch, T., Chen, D., Gao, J., Immerzeel, W., Piao, S., Su, F., Thompson, L., Wada,
644 Y., Wang, L., Wang, T., Wu, G., Xu, B., Yang, W., Zhang, G., and Zhao, P.: The imbalance
645 of the Asian water tower, Nature Reviews Earth & Environment, 3, 618-632,
646 <https://doi.org/10.1038/s43017-022-00299-4>, 2022.
- 647 Zemp, M., Jakob, L., Dussaillant, I., Nussbaumer, S. U., Gurmelen, N., Dubber, S., A, G.,
648 Abdullahi, S., Andreassen, L. M., Berthier, E., Bhattacharya, A., Blazquez, A., Boehm Vock,
649 L. F., Bolch, T., Box, J., Braun, M. H., Brun, F., Cicero, E., Colgan, W., Eckert, N., Farinotti,
650 D., Florentine, C., Floricioiu, D., Gardner, A., Harig, C., Hassan, J., Hugonnet, R., Huss, M.,
651 Jóhannesson, T., Liang, C.-C. A., Ke, C.-Q., Khan, S. A., King, O., Kneib, M., Krieger, L.,
652 Maussion, F., Mattea, E., McNabb, R., Menounos, B., Miles, E., Moholdt, G., Nilsson, J.,
653 Pálsson, F., Pfeffer, J., Piermattei, L., Plummer, S., Richter, A., Sasgen, I., Schuster, L.,
654 Seehaus, T., Shen, X., Sommer, C., Sutterley, T., Treichler, D., Velicogna, I., Wouters, B.,



- 655 Zekollari, H., Zheng, W., and The Gla, M. T.: Community estimate of global glacier mass
656 changes from 2000 to 2023, *Nature*, 639, 382-388, [https://doi.org/10.1038/s41586-024-08545-](https://doi.org/10.1038/s41586-024-08545-z)
657 [z](https://doi.org/10.1038/s41586-024-08545-z), 2025.
- 658 Zhang, G., Chen, W., and Xie, H.: Tibetan Plateau's Lake Level and Volume Changes From
659 NASA's ICESat/ICESat-2 and Landsat Missions, *Geophysical Research Letters*, 46, 13107-
660 13118, <https://doi.org/10.1029/2019GL085032>, 2019.
- 661 Zhang, G., Yao, T., Piao, S., Bolch, T., Xie, H., Chen, D., Gao, Y., O'Reilly, C. M., Shum, C.
662 K., Yang, K., Yi, S., Lei, Y., Wang, W., He, Y., Shang, K., Yang, X., and Zhang, H.: Extensive
663 and drastically different alpine lake changes on Asia's high plateaus during the past four
664 decades, *Geophysical Research Letters*, 44, 252-260, <https://doi.org/10.1002/2016GL072033>,
665 2017a.
- 666 Zhang, G., Yao, T., Shum, C. K., Yi, S., Yang, K., Xie, H., Feng, W., Bolch, T., Wang, L.,
667 Behrangi, A., Zhang, H., Wang, W., Xiang, Y., and Yu, J.: Lake volume and groundwater
668 storage variations in Tibetan Plateau's endorheic basin, *Geophysical Research Letters*, 44,
669 5550-5560, <https://doi.org/10.1002/2017GL073773>, 2017b.
- 670 Zhang, T., Wang, W., An, B., and Wei, L.: Enhanced glacial lake activity threatens numerous
671 communities and infrastructure in the Third Pole, *Nature Communications*, 14, 8250,
672 <https://doi.org/10.1038/s41467-023-44123-z>, 2023.
- 673 Zhang, Z., Li, X., Zhou, C., Zhao, Y., Zhao, G., and Tang, Q.: Linking ground ice and glacier
674 melting to lake volume change in the Dogai Coring watershed on the Tibetan Plateau, *Journal*
675 *of Hydrology*, 629, 130581, <https://doi.org/10.1016/j.jhydrol.2023.130581>, 2024.
- 676 Zhao, L., Zou, D., Hu, G., Du, E., Pang, Q., Xiao, Y., Li, R., Sheng, Y., Wu, X., Sun, Z., Wang,
677 L., Wang, C., Ma, L., Zhou, H., and Liu, S.: Changing climate and the permafrost environment
678 on the Qinghai–Tibet (Xizang) plateau, *Permafrost and Periglacial Processes*, 31, 396-405,
679 <https://doi.org/10.1002/ppp.2056>, 2020.

680